Hydrodynamic function of dorsal and anal fins in brook trout (Salvelinus fontinalis)

The Journal of Experimental Biology 210, 325-339
Published by The Company of Biologists 2007
doi:10.1242/jeb.02661

Hydrodynamic function of dorsal and anal fins in brook trout (*Salvelinus fontinalis*)

E. M. Standen* and G. V. Lauder
Museum of Comparative Zoology, Harvard University, 26 Oxford Street, Cambridge, MA 02138, USA
*Author for correspondence (e-mail: standen@fas.harvard.edu)

Accepted 21 November 2006

Summary

Recent kinematic and hydrodynamic studies on fish median fins have shown that dorsal fins actively produce jets with large lateral forces. Because of the location of dorsal fins above the fish's rolling axis, these lateral forces, if unchecked, would cause fish to roll. In this paper we examine the hydrodynamics of trout anal fin function and hypothesize that anal fins, located below the fish's rolling axis, produce similar jets to the dorsal fin and help balance rolling torques during swimming. We simultaneously quantify the wake generated by dorsal and anal fins in brook trout by swimming fish in two horizontal light sheets filmed by two synchronized high speed cameras during steady swimming and manoeuvring. Six major conclusions emerge from these experiments.

First, anal fins produce lateral jets to the same side as dorsal fins, confirming the hypothesis that anal fins produce fluid jets that balance those produced by dorsal fins. Second, in contrast to previous work on sunfish, neither dorsal nor anal fins produce significant thrust during steady swimming; flow leaves the dorsal and anal fins in the form of a shear layer that rolls up into vortices similar to those seen in steady swimming of eels. Third, dorsal and anal fin lateral jets are more coincident in time than would be predicted from simple kinematic expectations; shape, heave and pitch differences between fins, and incident flow conditions may account for the differences in timing of jet shedding. Fourth, relative force and torque magnitudes of the anal fin are larger than those of the dorsal fin; force differences may be due primarily to a larger span and a more squarely shaped trailing edge of the anal fin compared to the dorsal fin; torque differences are also strongly influenced by the location of each fin relative to the fish's centre of mass. Fifth, flow is actively modified by dorsal and anal fins resulting in complex flow patterns surrounding the caudal fin. The caudal fin does not encounter free-stream flow, but rather moves through incident flow greatly altered by the action of dorsal and anal fins. Sixth, trout anal fin function differs from dorsal fin function; although dorsal and anal fins appear to cooperate functionally, there are complex interactions between other fins and free stream perturbations that require independent dorsal and anal fin motion and torque production to maintain control of body position.

Key words: swimming, manoeuvring, locomotion, dorsal fin, anal fin, hydrodynamics, particle image velocimetry, stability, trout, *Salvelinus fontinalis.*

Introduction

A biomechanical trade off exists between stability and manoeuvrability in many animals, and fish are known to be particularly unstable in the roll axis (Webb, 2006). Compared to pitching and yawing instabilities, controlling for roll appears to be important as fish respond most consistently and quickly to perturbations that cause rolling (Webb, 2004). How fish control for rolling perturbations is unknown.

Previous experimental hydrodynamic studies have shown a large lateral component to the jets produced by the dorsal fin in bluegill sunfish *Lepomis macrochirus* and rainbow trout *Onchorynchus mykiss* (Drucker and Lauder, 2001a; Drucker and Lauder, 2005). The location of the dorsal fin above the rolling axis of the fish and behind its center of mass (CM) suggest that these lateral forces cause rolling torques that may lead to deleterious rolling instabilities during steady swimming. How do opposing fins, such as the anal fin located below the fish's CM, compensate for destabilizing torques that fins might produce during steady swimming? Kinematic studies on bluegill sunfish have shown that dorsal and anal fins have complimentary kinematic behaviour (Standen and Lauder, 2005) and it was hypothesized that dorsal and anal fins produce similar lateral jet forces during steady swimming.

The only hydrodynamic study that includes anal fins is the recent work using a transverse light sheet to assess hydrodynamic function of median fins in bluegill sunfish (Tytell, 2006). Tytell concluded that dorsal and anal fins produce streamwise vortices with thrust forces comparable to

those produced by the tail fin. The lateral component or temporal characteristics of jets from the anterior median fins were not addressed.

Fish fins have often been equated to flapping foils when considering their hydrodynamic function during swimming (Barrett et al., 1999; Zhu et al., 2002), and understanding the differences in hydrodynamic function between dorsal and anal fins begins with understanding the morphological and kinematic differences between fins. Fin shape, body location, kinematic oscillation and angle of attack are all important when determining hydrodynamic function. During swimming a propulsive wave moves down the fish's body driving median fin oscillation and forcing body and fins to oscillate at similar frequencies (Jayne et al., 1996). The fin's position on the body longitudinal axis will influence both the timing and magnitude of fin maximum amplitude. As the wave moves along the body its frequency remains constant and its amplitude increases. One would expect the changes in body wave mechanics to be reflected in the kinematics of median fins attached to the body. Although body oscillation is an important contributor to fin motion, each fin also has an independent set of musculature which can control the fin's movement pattern and shape (Standen and Lauder, 2005; Winterbottom, 1974).

The overall objective of this study is to understand the wake structures and resultant forces produced by trout dorsal and anal fins during steady swimming and manoeuvring. We use particle imaging velocimetry (PIV) with two horizontal light sheets to visualize the flow behind both dorsal and anal median fins simultaneously. We examine basic kinematic behaviours of the dorsal and anal fins during steady swimming at 0.5 and 1.0 $L\ s^{-1}$ as well as during manoeuvres. Our goal is to better understand how fish use their median fins to produce and balance forces required for swimming. We are particularly interested in forces acting around the fish's rolling axis. In this study we test two hypotheses. First that the anal fin, located below the rolling axis of the fish, produces equal and opposite torques compared to the dorsal fin, helping to minimize body perturbations in the roll axis during steady swimming. Second, that dorsal and anal fins produce different torques at different times during manoeuvres in order to change the fish's body position.

Materials and methods

Fish

We collected data using twelve brook trout *Salvelinus fontinalis* (Mitchill 1814) and analyzed in detail the four animals that had the most complete data sets. Fish were maintained in the laboratory, in a 1200 l circulating tank and kept on a 12 h:12 h light:dark photoperiod with a mean water temperature of 16°C (±1°C). The four individuals analyzed in this study had a mean total length (L) of 15.8 cm (range 13–17 cm; s.e.m.=0.90).

Behavioural and hydrodynamic observations

Trout swam in the centre of the working area (28 cm wide, 28 cm deep, 80 cm long) of a variable speed flow tank under conditions similar to those described in previous hydrodynamic work on both *Lepomis macrochirus* and *Onchorynchus mykiss* (Drucker and Lauder, 1999; Drucker and Lauder, 2001a; Drucker and Lauder, 2005; Standen and Lauder, 2005). Fish were recorded swimming steadily at 0.5 $L\ s^{-1}$ and 1.0 $L\ s^{-1}$. Fish also performed yawing turns while swimming at 0.5 $L\ s^{-1}$. Turns were elicited by dropping a wooden dowel along the side of the flow tank 15 cm lateral to the fish's head as in previous research (Drucker and Lauder, 2001b; Drucker and Lauder, 2005; Standen and Lauder, 2005). Care was taken to ensure the dowel did not disturb the flow visualized behind the fish. The swimming behaviours induced in this study are directly comparable to those studied on bluegill sunfish and rainbow trout (Drucker and Lauder, 2001a; Drucker and Lauder, 2001b; Drucker and Lauder, 2005; Standen and Lauder, 2005). We used two synchronized high-speed video cameras, one in dorsal and one in ventral view (Photron Fastcam, San Diego, CA, USA;

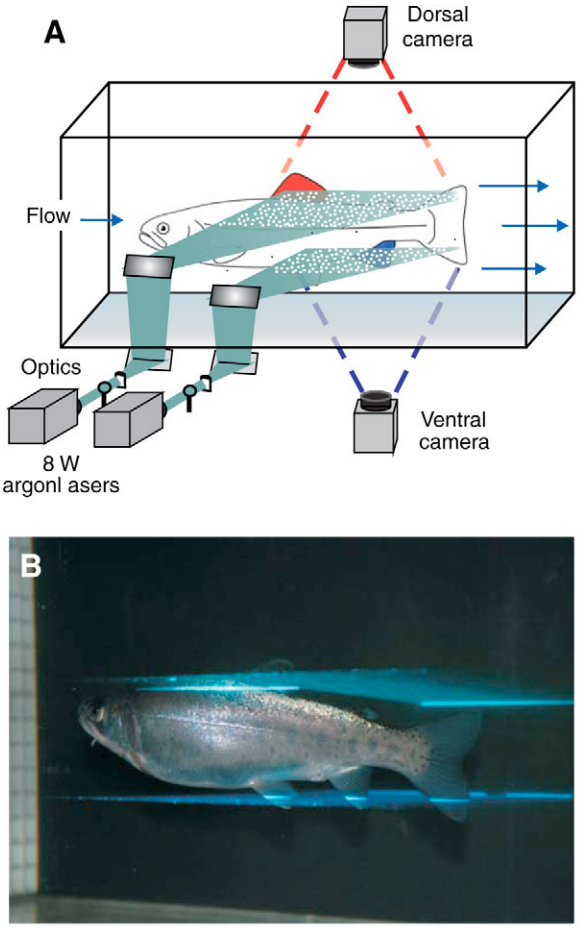

Fig. 1. Experimental apparatus. (A) Fish swam in a multi-speed flow tank with two horizontal light sheets projected simultaneously to illuminate the dorsal and anal fin wakes. High-speed cameras captured simultaneous dorsal and ventral views of the swimming fish. (B) Image of a trout swimming between the two light sheets.

1280×1024 pixels) operating at 250 frames s^{-1} (1/1000 s shutter speed) to visualize the movement patterns and wake structures of the dorsal and anal fin simultaneously (Fig. 1).

In all swimming trials the dorsal and anal fin wakes were visualized using particle imaging velocimetry (PIV). Two 8 W continuous-wave argon-ion lasers (Coherent Inc., Santa Clara, CA, USA) were focused into parallel light sheets (1–2 mm thick, 14 cm wide) that illuminated reflective micro particles suspended in the flow tank. The two laser sheets were simultaneously projected onto the swimming fish such that one sheet horizontally transected the dorsal fin and the second sheet horizontally transected the anal fin (Fig. 1). Particle movement caused by dorsal and anal fin motion was captured by imaging each laser light sheet with the high-speed video cameras (Fig. 1).

Camera calibration and dual light sheet interaction assessment

Dorsal and ventral camera images were calibrated using a full-field flat plate with clearly marked regularly spaced points. This image was used by DaVis software (DaVis 7.0.9, LaVision Inc., Göttingen, Germany) to correct for distortion of the camera lens and reshaped the video image to correct for parallax. All videos were analyzed using corrected video images.

Dorsal cameras were also tested to ensure that laser light from the ventral sheet did not register on the dorsal image and *vice versa*. A mechanical foil flapping back and forth was used to create turbulence in one light sheet and video images were analyzed for particle movement in both light sheets. In both cases the undisturbed light sheet had significantly lower mean vector magnitudes in the area corresponding to disturbance in the opposite light sheet (*t*-test, N=80, P<0.0001). The undisturbed mean vector magnitudes did not differ from free stream flow (*t*-test, N=80, P=0.36).

Morphological measurements

Fish fins were measured using ImageJ software to calculate fin area, aspect ratio and fin metrics. Fin area was described in two ways: total fin area was the full surface area of each fin and free fin area was the area of the fin located downstream of the posterior attachment of each fin. Free fin area allowed us to take into consideration the surface area differences between the most active portions of each fin. Aspect ratio (AR) was calculated using the equation AR=(span^2/area), where span is the height of the fin from trailing edge attachment to the leading edge tip and area is total fin area. Measuring height and width this way most accurately describes fin shape during swimming. We also measured fin free body edge, which is the portion of the fin's edge that continues along the body from the posterior attachment of the fin but is free from the body. Finally we calculated the ratio of fin heave amplitude to chord length (h/c) where chord is the fin width from leading edge attachment to trailing edge tip, a useful description of foil movement that influences wake morphology (Anderson et al., 1998; Hover et al., 2004).

Kinematic and hydrodynamic measurements

To quantify the temporal and spatial patterns of fin movement, video sequences were analyzed using a custom digitizing program in Matlab (version 6.5.1, Mathworks, Natick, MA, USA). For each of four fish we tracked the movement of dorsal and anal fins during five consecutive tailbeats of steady swimming at 0.5 $L\,s^{-1}$ and 1.0 $L\,s^{-1}$ and during yawing manoeuvres at 0.5 $L\,s^{-1}$. The mediolateral excursion (kinematic excursion) of dorsal and anal fins was quantified at 4 ms intervals by digitizing the trailing edge of each fin where it was transected by the light sheet. In addition, body excursion was quantified by digitizing the point where the dorsal and anal fin leading edges contacted the body. These data allowed full kinematic analysis of each fin. In this paper we focus on the magnitude and timing differences between fins during swimming.

Calculating phase lag

Because of their different positions along the body, dorsal and anal fins in trout oscillate out of phase. Based on this morphology we calculate the expected kinematic phase lag between fins by dividing the known distance between fins by body wave speed. Similarly, expected kinematic phase lag is calculated for each dorsal and anal fin trailing edge relative to the point on the body marked by the leading edge attachment of the anal fin. We can then compare the expected phase lag with what we observe the fins to do in swimming fish. This observed kinematic phase lag is the measured phase lag between dorsal and anal fin peak oscillations as well as between each fin and the point on the body marked by the leading edge attachment of the anal fin. The phase lags between peak lateral jet velocities for each fin are also calculated and compared with the observed kinematic phase lag between fin trailing edges. All phase lags are calculated as percent of full tailbeat cycle based on the fish's body wave.

Fins as foils: calculating their trajectories

Heave and pitch are important variables to consider when describing the behaviour of a flapping foil. Fin heave for both dorsal and anal fins (h_d and h_a) was defined by body oscillation at the leading edge of each fin. This measurement takes into consideration the body's function as a driving oscillatory force on the fins. Pitch angle (θ_d and θ_a) of each fin was described as the angle between the line from leading to trailing edge of each fin and the free stream flow. Phase angle (ψ_d and ψ_a) was defined as the lag between fin heave and pitch and helps define flow structure around a flapping foil. Angle of attack (α) was calculated as $\alpha(t)$=–arctan[$h(t)/U$]–$\theta(t)$, where U was the free stream flow velocity and t was time (s). Fin velocity (u_d and u_a) was calculated as the derivative of fin trailing edge kinematic excursion. Body velocity (u_{db} and u_{ab}) was calculated as the derivative of body kinematic excursion. Strouhal number (St) was calculated for each fin by the equation St=fA/U, where f is the fin trailing edge frequency and A is the kinematic excursion from peak to peak of fin trailing edge.

Hydrodynamic flow visualization

General patterns of water flow in the wake of dorsal and anal fins were established by reviewing 130 particle image velocimetry (PIV) video sequences performed by eleven fish. Detailed quantitative analysis was done on sequences where fish swam steadily for prolonged periods (N=5 fin beats per behaviour) or during manoeuvres (N=4 fin beats per behaviour).

PIV video sequences were analyzed in two different time scales: time averaged and instantaneous. The time averaged hydrodynamic analysis was comparable to previous PIV studies (Drucker and Lauder, 2001a; Drucker and Lauder, 2005) where flow velocities, angles and forces in the wake were calculated based on stroke averaged variables. The duration of the propulsive movement, τ, was calculated as the time taken to complete a half fin beat, in other words, to move the fin from maximum left excursion to the maximum right excursion. Only left to right propulsive movements were used in this study to avoid contaminating PIV analysis with bright areas on the video image produced by the ventral body surface. In this manner, τ was calculated for each right side stroke (for each individual, N=5 for each steady swimming sequence and N=4 for manoeuvres). Our stroke-averaged approach used a single video frame at maximum jet formation to calculate average jet force produced by each fin stroke and gave us an average hydrodynamic description of simultaneous dorsal and anal fin wakes that can be compared with results from earlier PIV studies (Drucker and Lauder, 2001a; Drucker and Lauder, 2005; Lauder et al., 2002). In contrast, for the instantaneous hydrodynamic analyses we calculated jet velocities and angles in each PIV video frame every 4 ms synchronized with the kinematic analysis, providing a more detailed temporal resolution of wake structure.

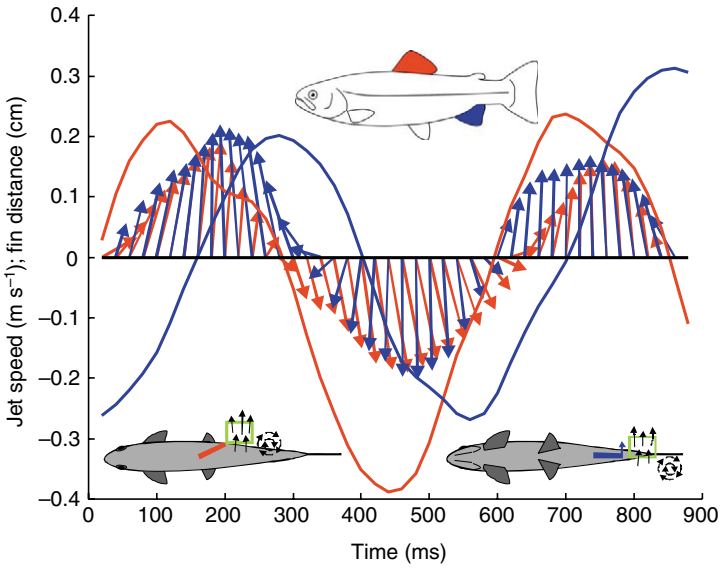

Fig. 2. Kinematic and hydrodynamic function of dorsal and anal fins during steady swimming at 0.5 L s^{-1}. Red and blue represent dorsal and anal fins, respectively. Solid lines represent fin kinematic oscillations over time. Red and blue arrows represent the direction and magnitude of fluid jets produced by fins. Green boxes on the fish indicate where the hydrodynamic data were sampled during fin oscillation.

Two-dimensional water velocity fields in the wake of trout were calculated from consecutive video frames (1280×1024 pixels) using DaVis 7.0.9 (LaVision Inc., Göttingen, Germany). We used sequential cross-correlation with an initial interrogation window size of 64×64 ending at 12×12 (6 passes, overlap 50%). Vector post processing was carried out using a median filter, which removed and iteratively replaced vectors greater than 2 times the root mean square of their neighbours. We measured horizontal plane flow fields that were 8–12 cm^2 and contained roughly 15 500 vectors (126×123 vectors). For the stroke-averaged wake calculations, vortices and jets found in the wake were used to calculate circulation, jet velocity and jet angle. For the instantaneous wake calculations, a small rectangular region (35×60 pixels) was fixed relative to the trailing edge of each fin (Fig. 2; 5 pixels downstream and extending 60 pixels to the right of the fin trailing edge and 35 pixels downstream) and was used to capture the wake represented by a constant area of water relative to the fin. As the fin moved the rectangular region also moved. The vectors contained within the region (N=60) were then used to calculate instantaneous jet velocities and angles through time as well as lateral and thrust components of the jets. All variables were collected and calculated using custom Matlab programs. Vectors that were located in the shadow of the fish or lay close to the illuminated body of the fish were misrepresentative of actual flow and not considered in the analysis. For all swimming behaviours the mean flow was subtracted from each vector matrix to reveal vortical structures in the wake and to allow measurement of jet flow structure and strength (Drucker and Lauder, 1999). Circulation was calculated as the line integral around a given vortex. Jet velocity was calculated as the average magnitude of vectors within the sample (instantaneous N=60; stroke-average N=153). Jet angle was calculated as the mean angle of these vectors relative to the streamwise heading of the fish, where a zero angle was along the midline of the fish facing backward and a 180° angle represents the heading of the fish (instantaneous jet angles N=60; stroke-averaged N=153).

In the present study, visualization of flow was restricted to the horizontal plain. Earlier PIV work has shown, using orthogonal light sheets, that the wake of median fins is a three-dimensional vortex ring (Drucker and Lauder, 1999; Drucker and Lauder, 2001a; Tytell, 2006). On this basis we determined the morphology of the vortex cores by measuring the distance between vortex rings within our horizontal light sheet. We assumed, based on previous studies (Drucker and Lauder, 2005; Spedding et al., 2003; Tytell, 2006) that the distance between consecutive vortices shed from the flapping fin represents the approximate width of the toroidal vortex ring. To calculate the height of the toroidal ring we used the height of the fin producing the paired vortices. The

radius (R) of the assumed toroidal vortex ring was calculated as the distance between the vortex cores plus the height of the median fin producing the vortices divided by 4. Ring momentum was calculated as the product of water density, mean vortex circulation and ring area. Ring area was πR^2. The time averaged wake force was then the momentum divided by the stroke period τ. This total force was resolved geometrically using the jet angle to determine the lateral and thrust components of force.

Statistics

Maximum fin excursion (mm), fin pitch (deg.), Strouhal number, jet magnitude (cm s^{-1}), mean jet angle (deg.), total and lateral jet forces (mN) and jet torques (mN cm) were analyzed using three-way partly nested ANOVAs with swimming speed and fin as fixed effects and fish as a random effect (Quinn and Keough, 2002). Fin velocity (cm s^{-1}), phase angle (deg.) and angle of attack (deg.) were analyzed using the same ANOVA, with steady swimming speed and fin as fixed effects and fish as a random effect. For steady swimming speeds during which the fish exhibited regular oscillatory swimming, expected kinematic phase lag due to fin and body position differences was compared with observed kinematic phase lag using three-way crossed ANOVAs where speed and type of phase lag were fixed effects and fish was a random effect. Comparisons of means within all ANOVAs were done using least square means (LSM) *post-hoc* tests. P-values of the LSM tests were subject to Bonferroni correction. Significance levels for all tests were based on initial P-values of <0.05 and all statistical tests were completed using SAS (version 9.1 TS Level 1M2 XP_Pro Platform). Measurements noted in the text are expressed as mean ± standard error of the mean (s.e.m.).

Results

Fin morphology

Dorsal and anal fins of brook trout *Salvelinus fontinalis* differ in all variables measured. Dorsal fin total area is larger than anal fin total area (mean total area: dorsal=3.90±0.27 cm^2, anal=3.01±0.11 cm^2). The free fin area of the anal fin (portion of fin downstream of posterior fin attachment to the body) is nearly twice the free area of the dorsal fin (mean free area: dorsal=0.87±0.21 cm^2, anal=1.76±0.21 cm^2). The free body edge of the dorsal fin is also longer than that of the anal fin (mean free body edge: dorsal=1.17±0.14 cm, anal=0.66±0.07 cm).

The aspect ratio (AR) of the anal fin is approximately 1.5 times larger than that of the dorsal fin (mean dorsal AR=1.78±0.37, anal AR=2.56±0.50). The heave to chord (h/c) ratio for the fins is greater for the anal fin compared with the dorsal fin and this ratio increases with speed (for values, see Table 1).

Moment arm of fin base to rolling axis of the fish is larger for the dorsal fin when compared with the anal fin (mean rolling axis moment arm: dorsal fin 1.34±0.07 cm, anal fin 0.97±0.03 cm).

Table 1. *Kinematic and hydrodynamic properties of fins during steady swimming and manoeuvres of brook trout*

	Kinematic excursion (mm)	Maximum trailing edge velocity (cm s^{-1})	Maximum lateral jet velocity (cm s^{-1})	Maximum angle of attack (deg.)	Body heave frequency (Hz)	Heave to chord ratio (h_0/c)	Pitch (deg.)	Phase angle Ψ (deg.)	Strouhal number (St)
Steady swimming at 0.5 L s^{-1}									
Dorsal fin	11.6±0.6	53.4±2.8	18±2	21.00±1.00	2.2±0.1	0.3±0.02	15.0±1.1	38.9±2.8	0.3±0.02
Anal fin	9.3±0.2	51.2±1.9	18±2	28.50±0.78	2.1±0.2	1.2±0.05	11.1±0.6	38.6±1.1	0.2±0.01
Dorsal body	1.9±0.2								
Anal body	4.6±0.3								
Steady swimming at 1.0 L s^{-1}									
Dorsal fin	10.1±0.5	77.8±4.0	13±2	18.38±0.91	2.9±0.3	0.4±0.02	12.1±0.8	34.7±1.3	0.2±0.01
Anal fin	9.9±0.3	67.7±3.3	18±2	32.00±1.00	2.9±0.3	1.7±0.06	15.0±0.6	28.0±0.7	0.2±0.01
Dorsal body	2.3±0.3								
Anal body	6.4±0.7								
Manoeuvres at 0.5 L s^{-1}									
Dorsal fin	10.4±1.1	47.0±2.5	16±3	26.83±1.96	3.5±0.8	0.5±0.08	19.7±1.8	–	0.2±0.03
Anal fin	9.6±0.7	51.1±2.6	18±2	33.94±2.18	2.5±0.4	1.2±0.1	16.3±1.4	–	0.2±0.02
Dorsal body	4.8±0.2								
Anal body	9.4±0.5								

Values are means ± s.e.m.
For kinematic variables, N>40 (a minimum of 10 half tailbeats for each of four fish at each speed).
For hydrodynamic variables, N>5 (a minimum of 5 half tailbeats for each of four fish at each speed).
Kinematic excursion is measured from peak lateral excursion on one side to peak lateral excursion on the other side of the fish.
Ψ is the phase lag between fin heave and pitch. Fin heave is defined by the oscillation of the body at the point of fin attachment.
$St = fA/U$, where f is heave frequency, A is kinematic excursion and U is swimming speed.

Whole fin kinematics

During steady swimming dorsal and anal fin movement is regular and oscillatory (Fig. 2). The body wave starts with minimal oscillation at anterior body positions and grows in amplitude as it passes toward the posterior portion of the body. Maximum fin and body excursion do not vary significantly between steady swimming speeds of 0.5, 1.0 $L\,s^{-1}$, and manoeuvres but do vary between fins (Table 1, ANOVA, N_{total}=403, $F_{(2,6)}$=0.22, P=0.81 and $F_{(3,9)}$=55.4, P<0.0001, respectively; the fin comparison includes dorsal and anal fin trailing edges and two points on the body relative to dorsal and anal fins). Overall, dorsal fins have larger excursions than anal fins (*post-hoc* LSM, P=0.0206), which have larger excursions than their respective body point (*post-hoc* LSM, P<0.0001 for both comparisons). Body oscillation amplitude at the dorsal fin is significantly less than body oscillation amplitude at the anal fin (*post-hoc* LSM, P<0.0001).

During oscillation the dorsal and anal fins accelerate as they cross the body midline and decelerate as they approach maximum excursion on either side of the body (Fig. 3). Maximum velocity of fin trailing edges during oscillation does not differ between steady swimming speeds or fins (Table 1; ANOVA, N_{total}=490, $F_{(1,3)}$=2.35, P=0.22 and $F_{(1,3)}$=0.35, P=0.60, respectively).

Dorsal and anal fin oscillations are driven by the body oscillation moving from anterior to posterior along the fish's body. The kinematic phase lag between dorsal fin and anal fin maximum excursion is what would be expected as a result of the fin position along the body's longitudinal axis (Table 2; ANOVA, $F_{(47,354)}$=184.87, *post-hoc* LSM, P=0.23). The observed kinematic phase lag between both fins and body are significantly different from what would be expected (*post-hoc* LSM, P<0.0001); both fins are phase shifted to reach maximum excursion later than expected.

Each fin has a heaving oscillation that is driven by the body where it attaches to the base of the fin. In addition, the trailing edge of each fin oscillates relative to its leading edge causing a pitch of the fin relative to free stream flow. The phase shift between the maximum heave and pitch for each fin is defined as the phase angle (ψ). Phase angle, ψ, between fin heave and pitch does not differ between speeds or fins (Table 1; ANOVA, N_{total}=178, $F_{(1,3)}$=3.49, P=0.16, and $F_{(1,3)}$=0.58, P=0.50, respectively), which means that the timing between the oscillatory patterns of heave and pitch for each fin foil are similar. For both fins, fin heave reaches maximum amplitude roughly 34° before fins reach maximum pitch. The body is already returning to the contra-lateral side of the fish, pulling the fin with it, when the fin tip is reaching maximum amplitude.

The magnitude of fin heave and pitch are also important in defining the angle of attack of each fin during oscillation. Maximum fin pitch does not differ between fins or speeds (Table 1, ANOVA, N_{total}=327, $F_{(1,3)}$=0.43, P=0.56 and $F_{(2,6)}$=3.19, P=0.11, respectively). Maximum excursion (or heave) of dorsal fins is larger than that of anal fins, influencing the relative angle of attack. Maximum angle of attack differs between fins (Table 1, anal>dorsal: ANOVA, N=266, $F_{(1,3)}$=31.03, P=0.01) but not between steady swimming speeds (ANOVA, N_{total}=266, $F_{(1,3)}$=0.02, P=0.89). Strouhal number (St) does not differ significantly between speeds or fins (Table 1, ANOVA, N_{total}=231, $F_{(2,6)}$=2.42, P=0.17, and $F_{(1,3)}$=1.83, P=0.27).

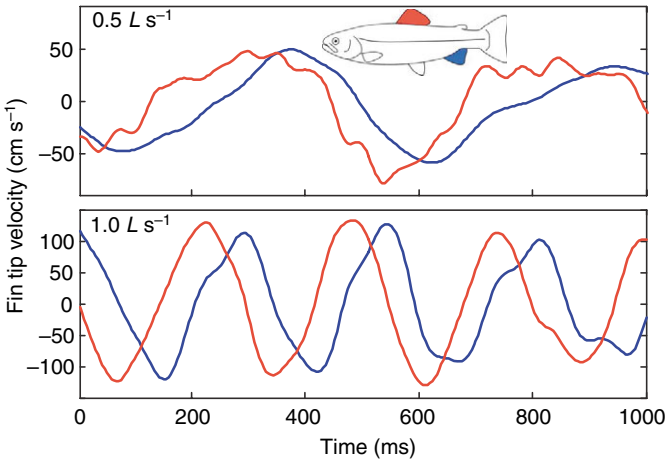

Fig. 3. Velocity of dorsal and anal fin tips during steady swimming at 0.5 and 1.0 $L\,s^{-1}$. Red and blue represent the dorsal and anal fins respectively. At 0.5 $L\,s^{-1}$ the anal fin maintains its smooth velocity sinusoid but the dorsal fin shows comparatively increased acceleration and deceleration and maintains fin maximum velocity for a longer proportion of the stroke cycle. The result is a plateau on the dorsal fin velocity graph containing a series of smaller peaks and troughs at high velocities during the cycle.

Hydrodynamics

During steady swimming, as fins beat from side to side, they produce jets with large lateral components to the same side of the body (Figs 2 and 4). Because the fins oscillate with a phase lag between them (kinematic phase lag) one would expect to see a similar phase lag between the jets produced by the fin's oscillation. The phase lag between dorsal and anal fin peak lateral jet velocity during steady swimming is significantly less than the kinematic phase lag between fins (Table 2, Fig. 2; ANOVA, $F_{(15,119)}$=14.87, *post-hoc* LSM, t=–8.13, P<0.001). Thus the timing of jet release from fin trailing edges relative to fin kinematic oscillation is different between dorsal and anal fins (Fig. 4). Maximum velocity of the lateral portion of these jets is similar between fins and swimming speeds (Table 1, ANOVA, N_{total}=113, $F_{(1,3)}$=1.87, P=0.26, and $F_{(2,6)}$=0.13, P=0.88). As a result, as the dorsal fin reaches maximum excursion the jet remains in close contact with the fin tip with little or no formation of a stop/start vortex (Fig. 4A). As the dorsal fin begins to return to the fish's midline, the jet reaches maximum lateral velocity (Fig. 4B). Over the same period of time the anal fin completes the formation of the previous stroke's stop/start vortex and a strong lateral jet is already forming off the anal fin trailing edge (Fig. 4A,B). Before the anal fin reaches maximum excursion (Fig. 4C) the lateral component of its jet reaches peak velocity and once at

Table 2. *Kinematic excursion and lateral jet velocity phase lag*

Group	Observed kinematic phase lag	Expected kinematic phase lag	Observed *vs* expected phase lag; *post-hoc* LSM *P*-value	Lateral jet velocity phase lag	Observed kinematic *vs* jet phase lag; *post-hoc* LSM *P*-value
Steady swimming at 0.5 L s^{-1}					
Anal fin–dorsal fin	21.22±1.60	23.32±1.40	0.2298	16.97±2.37	0.0001*
Dorsal fin–body	–3.82±1.45	–9.10±1.02	0.0001*		
Anal fin–body	17.56±0.75	13.98±0.59	0.0001*		
Steady swimming at 1.0 L s^{-1}					
Anal fin–dorsal fin	28.51±1.51	23.94±0.90	0.2298	9.07±1.95	0.0001*
Dorsal fin–body	–6.06±1.36	–9.80±0.90	0.0001*		
Anal fin–body	22.35±1.25	14.15±0.51	0.0001*		
Manoeuvres at 0.5 L s^{-1}					
Anal fin–dorsal fin	28.34±5.30	44.79±9.65	1.000	24.50±8.21	0.7758
Dorsal fin–body	–8.81±2.93	–20.71±4.82	1.000		
Anal fin–body	20.18±3.55	24.08±4.92	1.000		

Values are percent of tailbeat cycle (mean ± s.e.m.).
Kinematic phase lag, N=23–36 for each comparison group and evenly distributed between four fish.
Jet velocity phase lag, N=27–36 for each comparison group and evenly distributed between four fish.
LSM comparisons based on four ANOVAs (*significantly different P<0.5, Bonferroni corrected):
Steady swimming $ANOVA_{(1,5,3\ total=401)}$ phase lag = speed group fish speed×group speed×fish group×fish speed×group×fish.
Manoeuvring $ANOVA_{(5,3\ total=150)}$ phase lag = group fish group×fish.
Jets *vs* kinematics steady swimming $ANOVA_{(1,3\ total=134)}$ phase lag = group fish group×fish.
Jets *vs* kinematics manoeuvres $ANOVA_{(1,3\ total=54)}$ phase lag = group fish group×fish.

maximum excursion (Fig. 4D) the stop/start vortex is clearly being formed. During this time, the dorsal fin jet remains in close contact with the dorsal fin, and the stop/start vortex of the dorsal stroke starts to form at the point of anal fin maximum excursion (Fig. 4D).

Development of shear layers also appears to differ between dorsal and anal fins (Fig. 5). During dorsal fin oscillation a shear layer develops along the fin's advancing side. This shear layer rolls up into a strong vortex, the stopping vortex of one stroke being the starting vortex of the next (Fig. 5). In contrast, the anal fin appears to have a larger unstable shear layer that tends to roll up into two smaller vortices of the same sign; one vortex acting as stopping vortex for the previous stroke and the other acting as starting vortex for the next stroke (Fig. 5).

Although the anal fin jet appears to be more lateral in direction during jet formation compared with the dorsal fin (Fig. 5) there is no difference in time averaged mean jet angle between fins or speeds (Table 3; ANOVA, N_{total}=111, $F_{(1,3)}$=0.44, P=0.55, and $F_{(2,6)}$=0.53, P=0.61). Time averaged total jet forces do not differ between speeds or fins (Table 3; ANOVA, N_{total}=88, $F_{(2,6)}$=4.13, P=0.07 and $F_{(1,3)}$=1.62, P=0.29). The majority of the forces produced by both fins are lateral and, as would be expected, the time averaged lateral component of jet forces also do not differ between speeds or fins (Table 3; ANOVA, N_{total}=88, $F_{(2,6)}$=1.01, P=0.42 and $F_{(1,3)}$=1.81, P=0.27). The time averaged torques produced along the rolling axis do not differ significantly between speeds or fins (Table 3; ANOVA, N_{total}=88, $F_{(2,6)}$=0.94, $P\geqslant$0.44 and $F_{(1,3)}$=0.85, P=0.85).

Manoeuvres

Both dorsal and anal fins are used during manoeuvres but their motions become far more variable than during steady swimming. Differences in oscillation pattern are noticeable during manoeuvres where fin oscillations may have multiple peaks during a single excursion event and are not symmetrical on the two sides of the trout (Fig. 6). Variation in excursion of fins during manoeuvres is far greater than during steady swimming (Table 1) and, although any statistical significance is hidden by this variation, maximum excursion during manoeuvres can differ between dorsal and anal fins (Fig. 6; ANOVA, N_{total}=403, $F_{(2,6)}$=0.22, P=0.81). Changes in oscillation pattern cause kinematic phase lag between dorsal and anal fins to be larger and more variable than during steady swimming (Table 2).

Jet formation during manoeuvres is also more variable with multiple peaks and asymmetrical magnitudes and direction (Fig. 6). The magnitude of lateral jet velocity is similar to that during steady swimming but jet timing shows a much larger phase lag between fins (Table 2). Often the dorsal fin is held in an extended maximum excursion toward the side from which the fish is moving (Fig. 7A,B,C). This motion produces a large starting vortex with a lateral jet that remains closely associated with the fin trailing edge while the body of the fish is pushed away from the jet (Fig. 7C). In this example, while the dorsal fin remains at maximum excursion, the anal fin continues its motion toward maximum excursion and its jet develops simultaneously with the dorsal jet. The variation between fin motion and jet timing is much greater during manoeuvres than during steady swimming.

During yawing manoeuvres the shear layers that develop around the fins appear to behave differently compared with steady swimming. In a lateral manoeuvre the fish body moves sideways through the water column away from the stimulus. For the purposes of this paper, the two sides of the fish will be described as the stimulus side and the away side. Large amounts of shear develop on the away side of the dorsal fin as it approaches and is held at maximum excursion toward the stimulus side. This shear results in a series of smaller vortices that form a line along the path of the fin (Fig. 8). Very little shear develops on the stimulus side of the fin, large vortex structures roll cleanly from the tip of the fin as it reaches maximum excursion (Fig. 8). During manoeuvres the anal fin tends to have shear layers develop on both sides of the fin each layer rolling up into a single somewhat elongate vortex (Fig. 8).

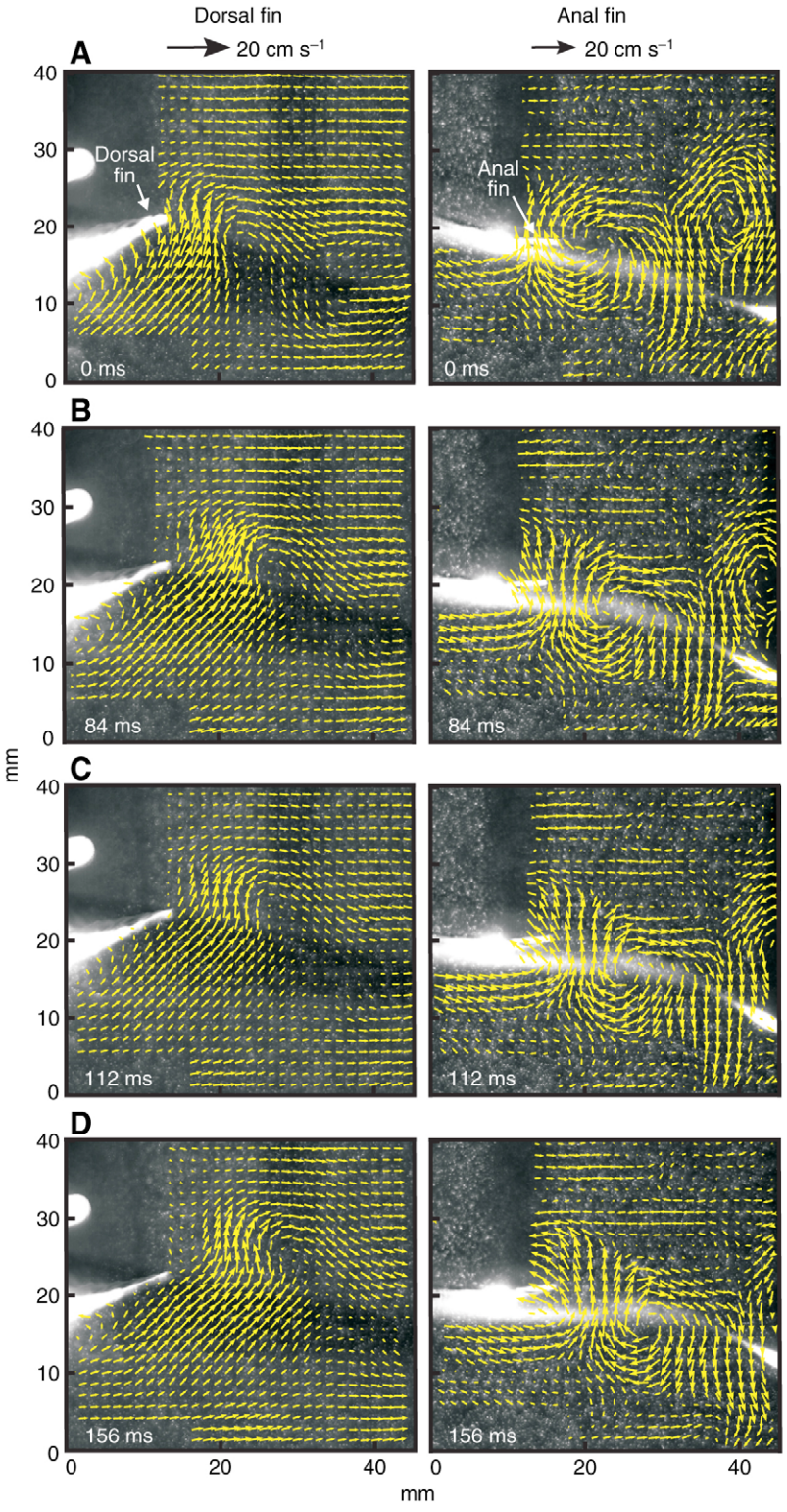

The extent to which the body is driving the fins during a manoeuvre can be seen with the increase in body amplitude and frequency during manoeuvres (Table 1). The change in heave increases the angle of attack of dorsal and anal fins during manoeuvres and the change in body wave frequency affects overall jet shedding during the manoeuvre. Jets produced by dorsal and anal fins during manoeuvres do not differ in force between fins (both lateral and total; ANOVA, N_{total}=88, $F_{(1,3)}$=1.81, P=0.27 and $F_{(1,3)}$=1.62, $P\geqslant$0.07, respectively) or from jets produced during steady swimming (both lateral and total; ANOVA, N_{total}=88, $F_{(2,6)}$=1.01, P=0.42 and $F_{(2,6)}$=4.13, $P\geqslant$0.07, respectively). Jet angle during manoeuvres does not differ between fins or from jet angles during steady swimming (Table 3; ANOVA, N_{total}=111, $F_{(1,3)}$=0.46, P=0.55 and $F_{(2,6)}$=0.53, P=0.61). Torque produced by dorsal and anal fins along the rolling axis does not change in magnitude during manoeuvres between fins or compared with steady swimming (Table 3; ANOVA, N_{total}=88, $F_{(1,3)}$=0.04, P=0.85 and $F_{(2,6)}$=0.94, $P\geqslant$0.44).

Discussion

How do fish balance rolling torques produced by their fins during swimming or imposed by external flow perturbations? In this study we use brook trout *Salvelinus fontinalis* to confirm that anal fins, located below the fish's rolling axis, produce equal and opposite torques compared to

Fig. 4. Simultaneous development of dorsal and anal fin jets in brook trout swimming at 0.5 L s^{-1}. (A) Dorsal fin at peak amplitude. Due to its location forward on the body the dorsal fin reaches maximum excursion before the anal fin. (B) Dorsal fin peak jet velocity. Peak jet formation by the dorsal fin occurs just after maximum kinematic excursion. (C) Anal fin at peak jet velocity, and (D) anal fin at peak amplitude. Peak jet formation by the anal fin occurs prior to maximum anal fin excursion resulting in a shorter maximum jet phase lag than would be expected from the kinematic phase lag seen between dorsal and anal fins. Note that x and y axes represent the scale of the video image.

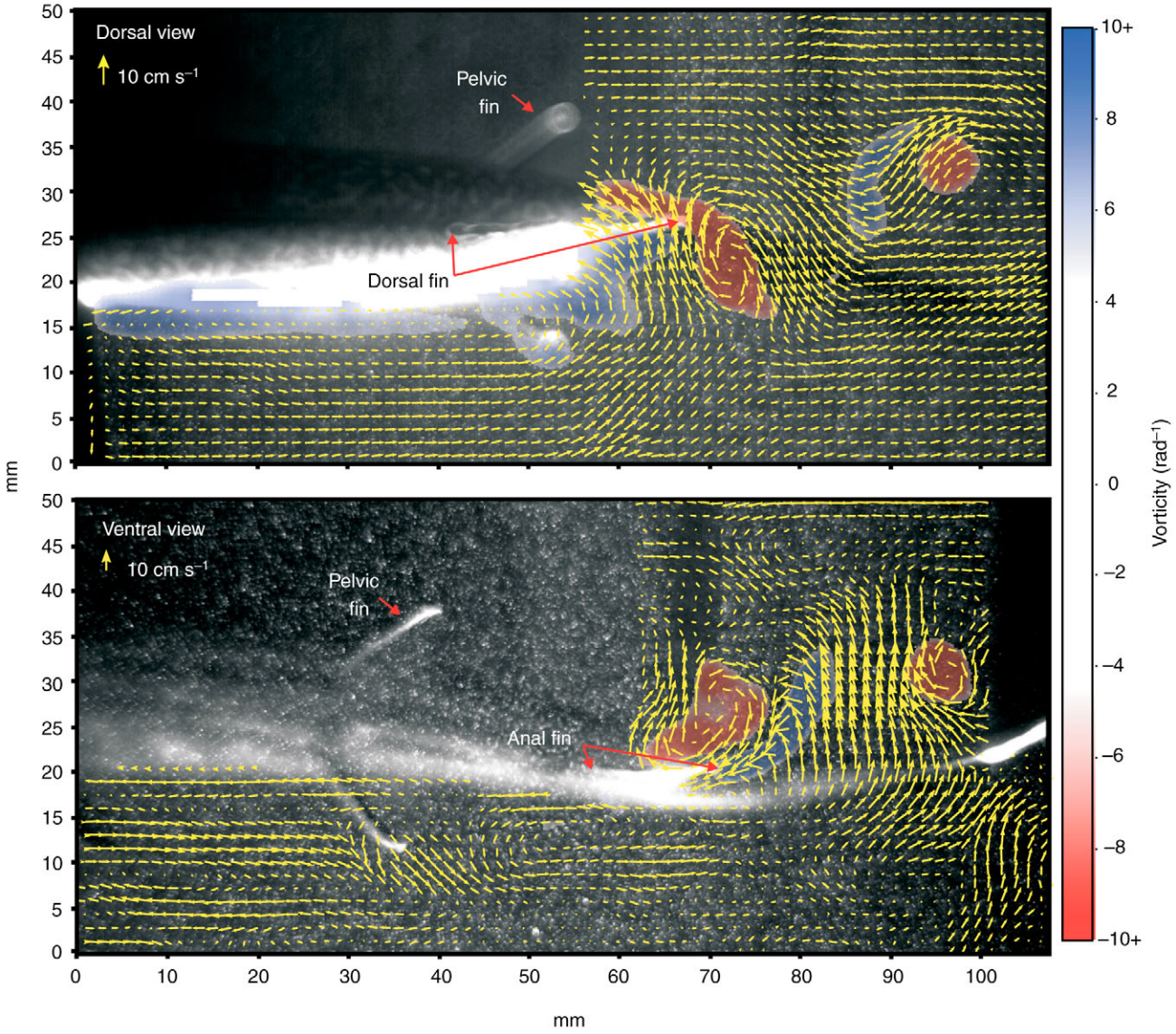

Fig. 5. Dorsal and anal fin vorticity and vector plots during steady swimming at 0.5 L s^{-1}. Top panel shows the dorsal fin with formation of trailing vortices during fin oscillation. Flow between the vortex centers shows jets to either side of the fish during a complete tail beat cycle. Bottom panel is the ventral view showing the anal fin producing shear flow on either side of the fin during the stroke. These shearing regions roll up and form elongated vortex cores. Both images reveal that shear build up along the side of fins develops long before the vortex is actually shed from the fin. Vectors have been removed from the image where they were disrupted by the shadow of the fish. Note that x and y axes represent the scale of the video image.

dorsal fins, located above the fish's rolling axis. This confirms that the anal fin helps minimize body perturbations in the roll axis during steady swimming. We also describe dorsal and anal fin function during manoeuvres and put forth the hypothesis that dorsal and anal fins, although sharing some functions, have distinctive functional repertoires.

Kinematic behaviour of brook trout dorsal and anal fins

In this study we found that brook trout oscillate their dorsal fin with a similar amplitude and frequency as rainbow trout (Drucker and Lauder, 2005). The anal fin also oscillates with each tail beat, and sends fluid jets to the same side as the dorsal fin, supporting our hypothesis that the anal fin acts in concert with the dorsal fin to balance fin torques. Fin oscillation and amplitude is influenced by two main factors. First, body wave oscillation drives the heave motion of fins, contributing directly to fin amplitude. Second, intrinsic fin musculature allows fine control of fin surface stiffness and movement. Electromyographic (EMG) recordings of dorsal fins in bluegill shows that dorsal fin musculature is active during swimming (Jayne et al., 1996). EMG data do not exist for trout median fins. However, we argue that differences in amplitude between fins suggests median fin oscillation may be actively controlled, and not a passive result of body oscillation (Table 1).

Table 3. *Time averaged mean circulation, vorticity, jet force, jet angle and torque for brook trout*

	Max circulation ($cm^2\ s^{-1}$)	Max vorticity ($rad\ s^{-1}$)	Max total jet force (mN)	Max lateral jet force (mN)	Mean jet angle (deg.)	Max rolling torque (mN cm)	Net dorsal and anal fin torque (mN cm)
Steady swimming at 0.5 $L\ s^{-1}$							
Dorsal fin	8±2	6.1±0.7	0.4±0.1	0.4±0.1	108.09±11.8	0.5±0.2	
Anal fin	8±2	6.6±0.5	0.7±0.2	0.6±0.2	93.5±10.3	0.6±0.1	0.2±0.1
Steady swimming at 1.0 $L\ s^{-1}$							
Dorsal fin	9±1	10.9±0.6	0.7±0.2	0.6±0.2	109.7±13.6	0.7±0.2	
Anal fin	8±2	7.9±0.9	1.2±0.4	1.0±0.4	111. 8±14.7	1.0±0.4	0.3±0.3
Manoeuvre at 0.5 $L\ s^{-1}$							
Dorsal fin	10±0.6	6.7±0.9	0.8±0.1	0.7±0.2	107.9±14.2	0.9±0.2	0.3±0.3
Anal fin	7±1	6.0±0.3	0.7±0.2	0.6±0.2	88.5±15.4	0.5±0.1	

Values are mean ± s.e.m., N=12–20. Net torque values are calculated by subtracting dorsal and anal fin rolling torque. The smaller roll torque value is subtracted from the larger and differences are listed in the row of the fin contributing greater torque.

Dorsal fins have larger amplitudes compared with anal fins and both fins have amplitudes greater than their adjacent body point (Table 1). As a propulsive wave moves down a fish's body the wave amplitude gets bigger (Lauder and Tytell, 2006). Thus, if completely passive, we would expect the anterior dorsal fin to have smaller amplitude compared with the more posterior anal fin. This is not the case. Despite the body amplitude being 2.5–2.7 times larger at the anal fin than at the dorsal fin, the anal fin has 0.8–0.97 times smaller amplitude than the dorsal fin. Dorsal fin amplitude exceeds that of the body by nearly 1 cm compared with anal fin amplitude, which exceeds that of the body by not quite 0.5 cm. Both dorsal and anal fins appear to be using intrinsic fin musculature to control fin amplitude independent of body oscillation but in different ways: we propose that the dorsal fin is actively augmenting its oscillation while the anal fin is actively dampening oscillation amplitude.

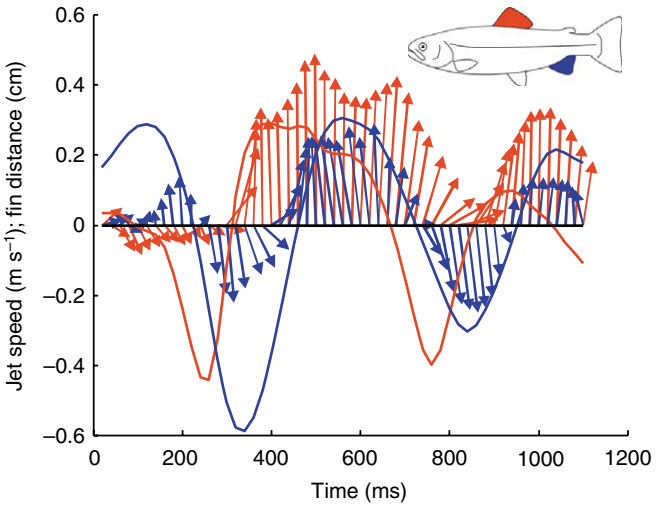

Fig. 6. Kinematic and hydrodynamic function of dorsal and anal fins during manoeuvring at 0.5 $L\ s^{-1}$. Red and blue represent dorsal and anal fins, respectively. Solid lines represent fin kinematic oscillations over time. Red and blue arrows represent the direction and magnitude of fluid jets produced by fin.

Hydrodynamic function of brook trout dorsal and anal fins

Jet formation by both dorsal and anal fins in brook trout appears to develop in a manner similar to that of the body wake produced by swimming eels. Vortex formation behind a swimming eel has been described in terms of primary and secondary vortices of similar rotational direction (Tytell and Lauder, 2004). Similar to eel swimming, although less pronounced, a primary vortex is formed by dorsal and anal fins at maximum excursion when the fin is changing direction, and is known as the stop/start vortex. Later in the stroke, as the shear along the fin surface begins to roll up, the secondary vortex is formed. Although in eels this process produces two or more distinct vortex structures, in the brook trout an elongate vortex with two rotation centers appears to form (Fig. 5). Although this rolling up of shear is present in both dorsal and anal fins it is more pronounced in the anal fin and can produce completely separate primary and secondary vortices as seen in eels.

Dorsal and anal fins produce similar lateral jets (dorsal above and anal below the trout's rolling axis; Table 3, Figs 2, 4, 5), confirming the hypothesis (Standen and Lauder, 2005) that dorsal and anal fin forces help balance each other during steady swimming. Of interest is the difference in observed kinematic phase lag between fins, and the phase lag seen between jets produced by those fins. Dorsal and anal fins oscillate together but with a kinematic phase lag of 21.22±1.60% tailbeat cycle at 0.5 $L\ s^{-1}$ and 28.51±1.51% tailbeat cycle at 1.0 $L\ s^{-1}$. These kinematic phase lags are what would be expected as determined from body wave speed and fin location along the fish's longitudinal axis. Interestingly, phase lag between the maximum lateral components of the jets produced by each fin is much smaller (16.97±2.37% tailbeat cycle at 0.5 $L\ s^{-1}$ and 9.07±1.95% tailbeat cycle at 1.0 $L\ s^{-1}$). It appears that morphological and kinematic properties of dorsal and anal fins cause them to shed vortices at slightly different points in their

oscillation cycle. This allows the lateral force produced by each fin to correspond more closely in time, reducing rolling torque imbalances.

Shape as well as heave and pitch differences between fins may account for the differences in timing of jet shedding. An important factor that influences the wake of a flapping foil is the formation and timing of the leading edge vortex (LEV) (Anderson et al., 1998; Dickinson et al., 1999). The LEV forms as the foil oscillates away from maximum excursion at high angles of attack. The LEV is shed with each stroke and interacts with the returning foil on the subsequent stroke. When the LEV is shed determines where it intercepts the chord wise axis of the returning foil influencing trailing edge vortex (TEV) shedding time and determining jet release from the fin. For example, a LEV that is shed late hits the returning foil close to its leading edge and will take longer to induce shedding of the TEV (Anderson et al., 1998); however, a LEV that is shed early, encounters the returning foil close to the trailing edge and helps induce early shedding of the TEV. We hypothesize that the trout anal fin is shedding its LEV early causing early shedding of the TEV.

Angle of attack, heave to chord ratio and aspect ratio are important in determining vortex structures, including LEV, surrounding a rigid flapping foil in mid to high Reynolds number regimes (Anderson et al., 1998; Read et al., 2003; Taylor et al., 2003). Although these variables can be used to predict vortex structures in wakes it is difficult to determine precisely the independent effects of each of the above variables on the timing of vortex shedding from a flapping foil. We have quantified the above hydrodynamic variables for each fin to determine how the fins may differ, and to explain the behaviour and timing of vortex structures behind the fins. We propose three mechanisms that may be working independently or together to produce different jet timing between dorsal and anal fins. First, the relationship between foil heave and pitch may affect vortex formation around the foil influencing jet release. Second, fin shape and amplitude of oscillation may alter jet formation and wake structure. Third, the direction of incident flow experienced by the foil affects the vortex wake of each fin. We now consider each of these three mechanisms in turn.

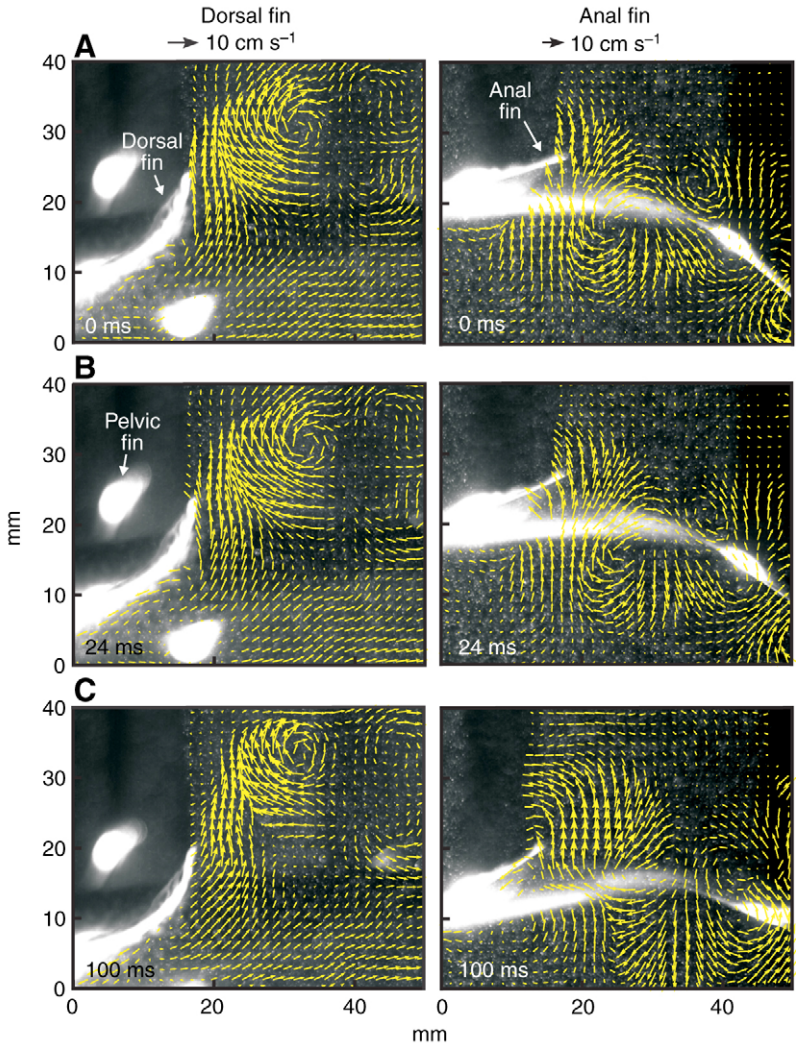

Fig. 7. Simultaneous dorsal and anal fin jet development in brook trout manoeuvring at 0.5 L s^{-1}. The fish is manoeuvring away from the stimulus located beyond the top of each image. (A) Dorsal fin at peak amplitude. (B) Dorsal fin peak jet velocity. The peak jet formation by the dorsal fin occurs just after maximum kinematic excursion with less phase lag than that seen in steady swimming. (C) Anal fin at peak amplitude and jet velocity. There is no phase lag between peak amplitude and peak jet velocity. Note that the pelvic fins appear as paired bright circular regions in the dorsal view because they intersect the ventral light sheet and reflect light into the dorsal camera. Similar pelvic fin reflections can be seen in the dorsal views shown in Fig. 6. Note that x and y axes represent the scale of the video image.

Foil pitch and heave: angle of attack

Dorsal and anal fins behave like pitching and heaving foils; body oscillation provides the fin's heave and intrinsic fin musculature drives the pitch motion changing the angle of the line from fin leading to trailing edge relative to free stream flow. Heave and pitch together determine the angle of attack of a foil because their motion produces the incident flow around the moving foil (Anderson et al., 1998; Read et al., 2003).

The fin's angle of attack determines both intensity and shedding time of the LEV (Anderson et al., 1998; Gopalkrishnan et al., 1994). At high angles of attack the LEV is large and unstable, shedding into the flow early. At lower angles of attack the LEV can be very small and attached to the leading edge of the foil. In our study, anal fin angle of attack is 1.4–1.8 times greater than dorsal fin attack angle [Table 1; mid range of angles chosen in Anderson et al. (Anderson et al., 1998)], possibly aiding in the early and stronger formation of

anal fin LEV compared with dorsal fin LEV (Gopalkrishnan et al., 1994), resulting in early jet production by the anal fin. This would explain the maximum lateral jet velocity occurring before the anal fin reaches maximum amplitude, as in Fig. 2.

Fin shape and amplitude

In addition to critical differences in angle of attack between fins, differences in fin shape and amplitude may contribute to wake differences. High aspect ratio (*AR*) foils are known to shed LEVs rapidly while lower foils develop spanwise flow, which stabilizes the LEV (Ellington, 1999). Hydrodynamic theory also suggests that large heave-to-chord ratio (*h*/*c*) with appropriate angles of attack causes flapping foils to form large LEVs that shed more easily (Anderson et al., 1998; Read et al., 2003). Brook trout median fins accord with hydrodynamic theory; not only is anal fin h_o/c four times greater than that of the dorsal fin (Table 1), but also anal fins are relatively high aspect ratio (*AR*, 2.56±0.50) and appear to shed LEVs early in the fin beat (soon after the fin begins to return from maximum excursion), while low *AR* dorsal fins (1.78±0.37) appear to shed more stable LEVs late, helping to explain the early release of anal fin TEV and lateral jet velocity.

Finally, differences in trailing edge shape between dorsal and anal fins may affect the stability and thus shedding frequencies of vortices produced by each fin [see Ellington's discussion of wing shape (Ellington, 1999)]. Dorsal fin trailing edge is triangular in shape with the apex of the triangle pointing downstream, while the anal fin trailing edge is a flat edge

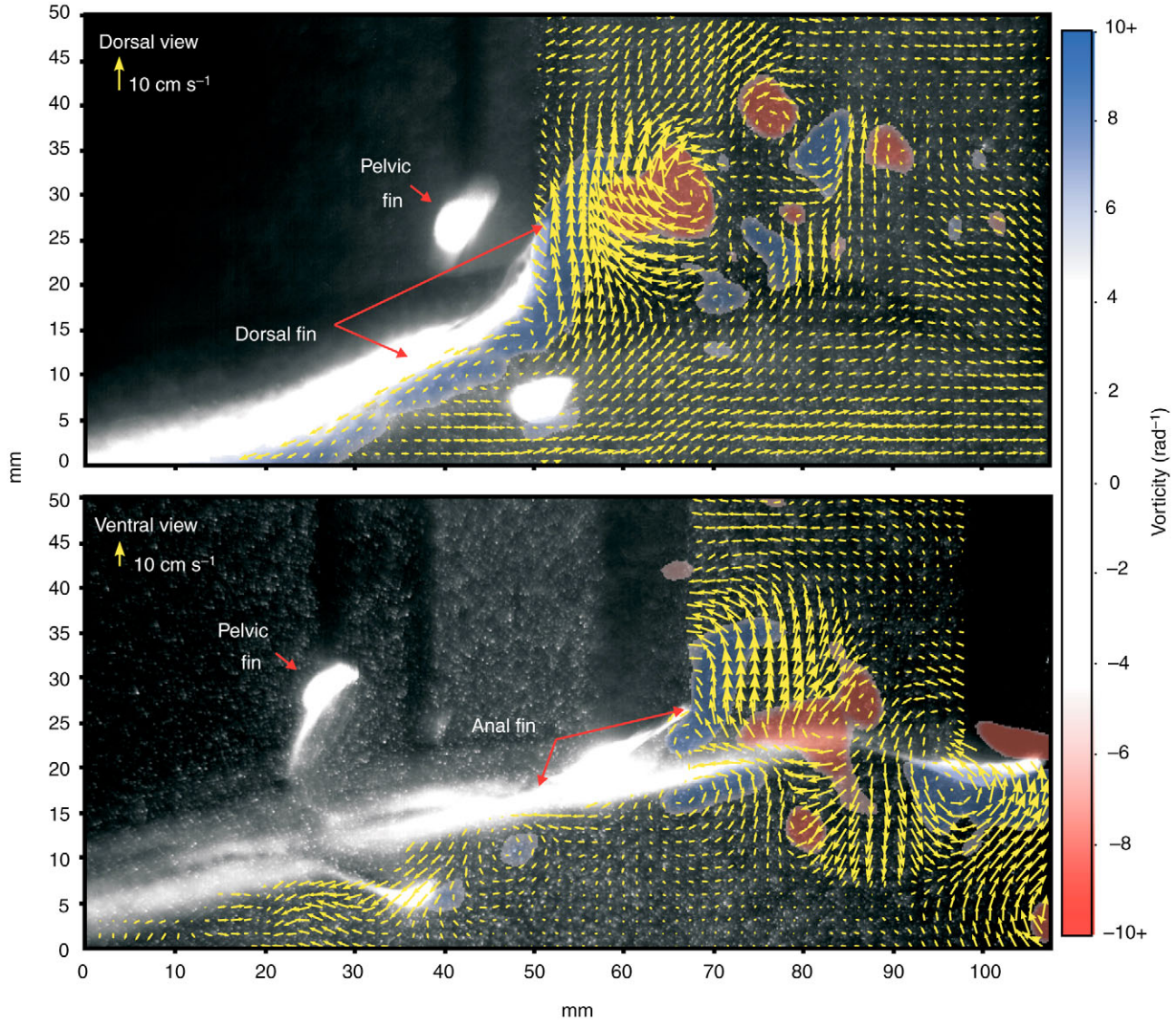

Fig. 8. Vorticity and vector plots during a manoeuvre at 0.5 L s^{-1}. The fish is manoeuvring away from the stimulus located beyond the top of each image. Top panel, dorsal fin during pause at maximum excursion as is commonly seen in lateral yawing manoeuvres. Bottom panel: anal fin returning to midline after the pause at maximum excursion. Shear layers can be seen on dorsal and anal fins. Formation of the second counterclockwise vortex appears early causing the formation of an imbalance in contralateral jet magnitude. Note that *x* and *y* axes represent the scale of the video image.

perpendicular to the direction of flow. Fin shape differences also influence the active area of the fin during oscillation. The dorsal fin is larger in total area than the anal fin (dorsal area=5.6±0.65, anal area=4.3±0.37 cm^2); however, when considering the posterior and most active portion of the fin (area downstream of the fin's posterior attachment), the anal fin area is larger than dorsal fin area (dorsal free area=1.25±0.34, anal free area=2.54±0.41 cm^2), a difference that may influence hydrodynamic function (i.e. flow acceleration) of fins during locomotion.

Incident flow conditions

Often the discussion of flapping foils and fish swimming is done in the context of relatively laminar, free stream flow at low Reynolds numbers (Blondeaux et al., 2005; Triantafyllou et al., 2000; Wolfgang et al., 1999; Zhu et al., 2002). However, the flow surrounding fish fins is not laminar due to disturbance of incident flow from obstacles in the environment and from upstream body and fin motion of the fish itself. Complex flow containing vortical structures that interact with flapping foils can dramatically affect the regular shedding of the foil's trailing edge vortices (Akhtar and Mittal, 2005; Gopalkrishnan et al., 1994). In brook trout, the anal fin is subject to more complex incident flow compared with the dorsal fin. In trout both sets of paired fins (pectoral and pelvic) are located ventrally on the body just upstream of the anal fin, and when swimming at lower speeds trout oscillate their paired fins for thrust production (Drucker and Lauder, 2003). Hydrodynamic analyses of the pectoral fins in trout show that at low speeds and hovering they shed vortices (Drucker and Lauder, 2003). Although the vortical structure of the pectoral fin wake may not stay intact to influence the anal fin as a regular vortex ring, it certainly adds turbulent structure to the flow interacting with the anal fin. In addition, video data (Fig. 5; E.M.S., unpublished data) show that the pelvic fin wake appears to provide semi-regular vortical flow to the anal fin. We suggest that these vortices or directional flow help initiate development and/or shedding of the leading edge vortex and thus enable the early formation of the trailing edge vortex, resulting in an early production of a lateral jet.

Effects of swimming speed and manoeuvres

Subtle differences in median fin kinematics exist among swimming speeds, although maximum fin trailing edge velocities are the same between speeds and fins; there is a difference in fin acceleration. At 1.0 $L\ s^{-1}$, dorsal and anal fin velocities oscillate in a smooth sinusoidal manner with relatively constant accelerations and decelerations and single peak velocities within each half finbeat. At 0.5 $L\ s^{-1}$ the anal fin maintains its smooth velocity sinusoid but the dorsal fin increases acceleration and deceleration and maintains fin maximum velocity for a longer portion of the stroke (Fig. 3). This results in a plateau on the dorsal fin velocity graph, which contains a series of smaller peaks and troughs at high velocities during the cycle (Fig. 3). This more constant velocity behaviour of the dorsal fin shortens the phase lag between fin peak velocities. Constant velocity throughout a greater portion of the stroke may also help stabilize the trailing edge vortex, resulting in a postponed jet release as well as allowing the smaller dorsal fin free area to operate at a higher velocity for longer adding more momentum to the flow over time. In contrast, the sharp accelerations and decelerations of the anal fin would be conducive to shedding vortices quickly. Low speeds may induce this change in dorsal fin behaviour in an effort to overcome difficulties in maintaining body position while swimming slowly.

There may be energetic consequences to swimming at slow speeds that are related, not to producing thrust, but to maintaining body position or stability (Webb, 2002; Webb, 2006; Webb and Fairchild, 2001). The subtle changes in velocity seen within the plateau of the dorsal fin velocity profile suggest that trout are fine-tuning fin movements to maintain body position at low speeds where energy use for stability outweighs that needed for thrust. At higher speeds this fine tuning control is not present, possibly because stabilization requirements drop when swimming velocities increase.

The plateau pattern of fin oscillation, velocity and acceleration is also common during manoeuvres (Fig. 6). Asymmetry between dorsal and anal fin amplitudes and resultant jets are extremely variable and make it difficult to summarize manoeuvres using mean values. The most telling measurements for manoeuvres are the large s.e.m. for each mean value. Trout can control dorsal and anal fins independently from one another, as has previously been seen in bluegill sunfish kinematics where fish controlled dorsal and anal fin shape and surface area differently during manoeuvres (Standen and Lauder, 2005). Standen and Lauder hypothesized that kinematic asymmetry produces unbalanced torques on the fish's body allowing for concise control of body position during a manoeuvre (Standen and Lauder, 2005); flow visualization of trout dorsal and anal fins during manoeuvres indeed show large differences in jet velocity and resultant torques (Table 3), supporting this hypothesis as well as the hypothesis put forth by the present paper that dorsal and anal fins have distinct functional repertoires.

Force, stability and rolling torques

Although mean velocity magnitudes of jets produced by dorsal and anal fins did not differ, estimating the size of each jet shows that anal fins produce jets with lateral forces nearly twice those of dorsal fins (Table 3). This large difference in force production would lead to roll instability if it were not for the fin's location relative to the fish's rolling axis.

Controlling body position requires balancing torques that act on the fish's body. Torque is the product of the position of force application and force magnitude. One must consider not only fin force production but also fin location when determining how fins are contributing to body control.

The centre of mass (CM) on a trout is located just below the lateral line anterior to the pelvic fins. The fish's rolling axis passes through the CM running cranio-caudally through the body. The dorsal fin is located above the trout's rolling axis

and the anal fin below. By comparing the moment arm or distance from the base of each fin to the rolling axis we can estimate the torque each fin is imposing on the body. The dorsal fin produces smaller forces and has a larger moment arm compared with the anal fin, indicating that rolling torques produced by dorsal fin and anal fin are roughly equal (at 0.5 L s^{-1} dorsal fin=0.5±0.2 mN cm, anal fin=0.6±0.1 mN cm; at 1.0 L s^{-1} dorsal fin=0.7±0.2 mN cm, anal fin=1.0± 0.4 mN cm; Table 3). There is high variation associated with torque production for both fins. This variation suggests that although torque production between fins is largely balanced, there may be times throughout each stroke that anal fin torques are larger than dorsal fin torques. This imbalance, although minor, suggests that although dorsal and anal fins appear to cooperate functionally, there are more complex interactions between other fins and free stream perturbations that influence torque production by the median fins.

We did not quantify pitching or yawing torques produced by dorsal and anal fins as a part of this analysis. It is clear from our data, however, that anal fins should be producing larger pitching and yawing torques compared to the dorsal fin. The anal fin's posterior location compared with the dorsal fin means it has a longer moment arm to both the trout's pitching and yawing axis which, along with its larger force production, suggests that torques produced by the dorsal and anal fins are not balanced in pitch or yaw. These imbalances may serve to compensate for unequal torque production by pectoral fins, pelvic fins, and asymmetrical caudal fin motion.

Median fin function in trout and bluegill compared

Fin oscillation kinematics in large part determines fin wake structures. Hydrodynamic studies of trout and bluegill have shown that oscillating dorsal fins produce jets with a large lateral component (Drucker and Lauder, 2001a; Drucker and Lauder, 2005; Tytell, 2006). A jet angle of 0° means the entire jet is producing only thrust force, while an angle of 90° produces a completely lateral force; jet angles of greater than 90° produce drag. The dorsal fin of bluegill sunfish has a mean jet angle of 62.4±1.8°, which contributed a considerable lateral force but also some thrust force during swimming (Drucker and Lauder, 2001a). In contrast, we found that the brook trout in our study produce dorsal and anal fin jets with angles greater than 90° (Table 3), suggesting that dorsal and anal fins are not contributing to thrust but produce drag and lateral forces. This difference in jet direction produced by median fins of bluegill and trout may point to a functional dichotomy between fishes; at slow speeds, dorsal and anal fins in trout may be used for stabilizing and braking while in bluegill they are used both for stabilization and thrust production.

Stability has not been the only function attributed to the dorsal fin of fishes. Dorsal fin jets produced by bluegill sunfish and rainbow trout have been shown to have a thrust component to their jet (jet angles of 62° and 75°, respectively) (Drucker and Lauder, 2001a; Drucker and Lauder, 2005). The downstream component of these jets has been hypothesized to contribute up to 12% of thrust in bluegill sunfish and 16% of thrust in rainbow trout (during steady swimming at roughly 1.0 L s^{-1}). A second study with bluegill, the only study including hydrodynamic analysis of anal fins, estimated that dorsal and anal fins combined produce a similar amount of thrust force compared with the caudal fin during steady swimming (Tytell, 2006). In contrast, this study shows that brook trout dorsal and anal fin jets do not appear to have a thrust component to their jets (jet angles of 110° and 112°, respectively; Table 3); in fact they contribute a drag wake to the fish during steady swimming at 0.5 and 1.0 L s^{-1}. Drucker and Lauder suggested the larger lateral jet direction found in rainbow trout compared with bluegill compensated for differences in roll stability due to body shape of the two fish (Drucker and Lauder, 2005). The laterally compressed body form of bluegill may resist roll more effectively than the elongate cylindrical form of rainbow trout. Trout thus may require more lateral force production to compensate for body roll moments induced by ambient perturbations in flow. Although this may explain the difference in median fin jet production between two very different body forms in fish (trout and bluegill), it is difficult to understand why there would be an even larger difference in jet direction between two species of trout (rainbow and brook), each with very similar body forms.

The drag component of the jets produced by dorsal and anal fins in brook trout may be serving two purposes. First, drag forces may help to maintain the heading of the fish, acting as a weather vane in the free stream flow. Second, fin drag may brake or slow and stabilize trout during swimming at very low speeds, acting as a brake while thrust is simultaneously produced by the body and tail. Subtle increases in caudal fin area and body depth in brook trout compared with rainbow trout may increase body caudal thrust production in brook trout, requiring them to increase stabilization and drag to maintain slow speed swimming. Also, jets produced by dorsal fins in brook trout are much weaker than those quantified in rainbow trout (for brook trout, see Table 3; rainbow trout, 0.5 L s^{-1}=0.62±0.16 mN, 1.0 L s^{-1}=2.20±0.51 mN (Drucker and Lauder, 2005), suggesting subtle fine tuning of torque production on the body for stabilization rather than strong propulsive hydrodynamic function.

A second method of thrust production through dorsal/caudal wake interaction has been suggested in both bluegill and rainbow trout (Drucker and Lauder, 2001a; Drucker and Lauder, 2005). Vortices shed from the dorsal fin can interact with the tail. If the timing of this vortex shedding is correct, dorsal vortices will join and strengthen same-sign vortices attached to the caudal fin, possibly increasing thrust (Drucker and Lauder, 2001a). The proximity of dorsal and anal fins to the caudal fin in bluegill sunfish suggests that vortex structures in the wake of either fin will remain intact and interact with the caudal fin. In trout, however, dorsal fins are located farther upstream on the fish's body and the vortex structures may decay before reaching the caudal fin. In trout, anal fins are posterior to dorsal fins, making them closer to the caudal fin, and possibly giving them a larger function in producing wakes

that can be utilized by the caudal fin to enhance thrust, as suggested as a function of the acanthopterygian dorsal fin (Drucker and Lauder, 2001a). Analysis of dorsal and anal fin wake effects on caudal fin thrust would be an intriguing next step in understanding the biomechanics of locomotion in trout.

We are grateful to all the people in the Lauder Lab. Thanks in particular to Jeremiah Alexander for looking after the animals. We also thank Silas Alban and Marcus Roper for valuable consultation regarding the fluid mechanics of flapping foils. Funding for this project was provided by NSF IBN0316675 to G.V.L.

References

Akhtar, I. and Mittal, R. (2005). A biologically inspired computational study of flow past tandem flapping foils. *AIAA Paper* **2005-4760**.

Anderson, J. M., Streitlien, K., Barrett, D. S. and Triantafyllou, M. (1998). Oscillating foils of high propulsive efficiency. *J. Fluid Mech.* **360**, 41-72.

Barrett, D. S., Triantafyllou, M. S., Yue, D. K. P., Grosenbaugh, M. A. and Wolfgang, M. J. (1999). Drag reduction in fish-like locomotion. *J. Fluid Mech.* **392**, 183-212.

Blondeaux, P., Fornarelli, F. and Guglielmini, L. (2005). Numerical experiments on flapping foils mimicking fish-like locomotion. *Phys. Fluids* **17**, 1-12.

Dickinson, M. H., Lehmann, F. O. and Sane, S. P. (1999). Wing rotation and the aerodynamic basis of insect flight. *Science* **284**, 1954-1960.

Drucker, E. G. and Lauder, G. V. (1999). Locomotor forces on a swimming fish: three-dimensional vortex wake dynamics quantified using digital particle image velocimetry. *J. Exp. Biol.* **202**, 2393-2412.

Drucker, E. G. and Lauder, G. V. (2001a). Locomotor function of the dorsal fin in teleost fishes: experimental analysis of wake forces in sunfish. *J. Exp. Biol.* **204**, 2943-2958.

Drucker, E. G. and Lauder, G. V. (2001b). Wake dynamics and fluid forces of turning maneuvers in sunfish. *J. Exp. Biol.* **204**, 431-442.

Drucker, E. G. and Lauder, G. V. (2003). Function of pectoral fins in rainbow trout: behavioural repertoire and hydrodynamic forces. *J. Exp. Biol.* **206**, 813-826.

Drucker, E. G. and Lauder, G. V. (2005). Locomotor function of the dorsal fin in rainbow trout: kinematic patterns and hydrodynamic forces. *J. Exp. Biol.* **208**, 4479-4494.

Ellington, C. P. (1999). The novel aerodynamics of insect flight: applications to micro-air vehicles. *J. Exp. Biol.* **202**, 3439-3448.

Gopalkrishnan, R., Triantafyllou, M., Triantafyllou, G. S. and Barrett, D. S. (1994). Active vorticity control in a shear flow using a flapping foil. *J. Fluid Mech.* **274**, 1-21.

Hover, F. S., Haugsdal, O. and Triantafyllou, M. S. (2004). Effect of angle of attack profiles in flapping foil propulsion. *J. Fluids Struct.* **19**, 37-47.

Jayne, B. C., Lozada, A. F. and Lauder, G. V. (1996). Function of the dorsal fin in bluegill sunfish: motor patterns during four distinct locomotor behaviours. *J. Morphol.* **228**, 307-326.

Lauder, G. V. and Tytell, E. D. (2006). Hydrodynamics of undulatory propulsion. In *Fish Biomechanics*. Vol. 23 (ed. R. E. Shadwick and G. V. Lauder), pp. 425-462. San Diego: Elsevier.

Lauder, G. V., Nauen, J. C. and Drucker, E. G. (2002). Experimental hydrodynamics and evolution: function of median fins in ray-finned fishes. *Integr. Comp. Biol.* **42**, 1009-1017.

Mitchill, S. L. (1814). The fishes of New York, described and arranged. *Trans. Lit. Phil. Soc. N. Y.* **1**, 1-28.

Quinn, G. P. and Keough, M. J. (2002). *Experimental Design and Data Analysis for Biologists*. Cambridge: Cambridge University Press.

Read, D. A., Hover, F. A. and Triantafyllou, M. S. (2003). Forces on oscillating foils for propulsion and maneuvering. *J. Fluid Struct.* **17**, 163-183.

Spedding, G. R., Rosen, M. and Hedenstrom, A. (2003). A family of vortex wakes generated by a thrush nightingale in free flight in a wind tunnel over its entire natural range of flight speeds. *J. Exp. Biol.* **206**, 2313-2344.

Standen, E. M. and Lauder, G. V. (2005). Dorsal and anal fin function in bluegill sunfish *Lepomis macrochirus*: three-dimensional kinematics during propulsion and maneuvering. *J. Exp. Biol.* **208**, 2753-2763.

Taylor, G. K., Nudds, R. L. and Thomas, A. L. R. (2003). Flying and swimming animals cruise at a Strouhal number tuned for high power efficiency. *Nature* **425**, 707-711.

Triantafyllou, M. S., Triantafyllou, G. S. and Yue, D. K. P. (2000). Hydrodynamics of fishlike swimming. *Annu. Rev. Fluid Mech.* **32**, 33-53.

Tytell, E. D. (2006). Median fin function in bluegill sunfish *Lepomis macrochirus*: streamwise vortex structure during steady swimming. *J. Exp. Biol.* **209**, 1516-1534.

Tytell, E. D. and Lauder, G. V. (2004). The hydrodynamics of eel swimming. I. Wake structure. *J. Exp. Biol.* **207**, 1825-1841.

Webb, P. W. (2002). Control of posture, depth, and swimming trajectories of fishes. *Integr. Comp. Biol.* **42**, 94-101.

Webb, P. W. (2004). Response latencies to postural disturbances in three species of teleostean fishes. *J. Exp. Biol.* **207**, 955-961.

Webb, P. W. (2006). Stability and maneuverability. In *Fish Biomechanics*. Vol. 23 (ed. R. E. Shadwick and G. V. Lauder), pp. 281-332. San Diego: Elsevier.

Webb, P. W. and Fairchild, A. G. (2001). Performance and maneuverability of three species of teleostean fishes. *Can. J. Zool.* **79**, 1866-1877.

Winterbottom, R. (1974). Descriptive synonymy of the striated muscles of the Teleostei. *Proc. Acad. Nat. Sci. Philadelphia* **125**, 225-317.

Wolfgang, M. J., Anderson, J. M., Grosenbaugh, M. A., Yue, D. K. P. and Triantafyllou, M. S. (1999). Near-body flow dynamics in swimming fish. *J. Exp. Biol.* **202**, 2303-2327.

Zhu, Q., Wolfgang, M. J., Yue, D. K. P. and Triantafyllou, M. S. (2002). Three-dimensional flow structures and vorticity control in fish-like swimming. *J. Fluid Mech.* **468**, 1-28.